Interaction of NH3 with Cu-SSZ-13 catalyst: a complementary FTIR, XANES and XES study

UNIVERSITÀ DEGLI STUDI DI TORINO

Interaction of NH_3 with Cu-SSZ-13 Catalyst: a Complementary FTIR, XANES and XES Study

Filippo Giordanino†,±, Elisa Borfecchia†,±, Kirill A. Lomachenko†,§, Andrea Lazzarini†,±, Giovanni Agostini‡, Erik Gallo‡, Alexander V. Soldatov§, Pablo Beato‖, Silvia Bordiga,†,±, Carlo Lamberti†,#,§*

† Department of Chemistry and INSTM Reference Center, University of Turin, via P. Giuria 7, 10125 Turin, Italy
± NIS Centre of Excellence, University of Turin, Italy
‡ European Synchrotron Radiation Facility, 6, rue Jules Horowitz, B.P. 220, F-38043 Grenoble cedex, France
‖ Haldor Topsøe A/S, Nymøllevej 55, 2800 Kgs. Lyngby, Denmark
CrisDI center of crystallography, University of Turin, Italy
§ Southern Federal University, Zorge street 5, 344090 Rostov-on-Don, Russia

AUTHOR INFORMATION

Corresponding Author

* E-mail: silvia.bordiga@unito.it

ABSTRACT

In the typical NH_3-SCR temperature range (100–500 °C), ammonia is one of the main adsorbed species on acidic sites of Cu-SSZ-13 catalyst. Therefore the study of adsorbed ammonia at high temperature is a key step for the understanding of its role in the NH_3-SCR catalytic cycle. We employed different spectroscopic techniques in order to investigate the nature of the different complexes occurring upon NH_3 interaction. In particular, FTIR spectroscopy revealed the formation of different NH_3 species, *i.e. (i)* NH_3 bounded to copper centers, *(ii)* NH_3 bounded to Brønsted sites, and *(iii)* $NH_4^+ \cdot n NH_3$ associations. XANES and XES spectroscopy allowed us to get an insight on the geometry and electronic structure of Cu canters upon NH_3 adsorption, revealing for the first time in Cu-SSZ-13 the presence of linear Cu^+ species in O_{fw}–Cu–NH_3 and/or H_3N–Cu–NH_3 configuration.

TOC GRAPHICS

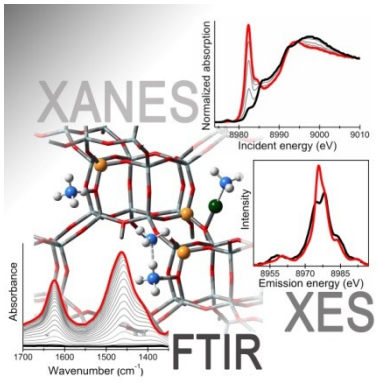

KEYWORDS

Cu-SSZ-13, NH_3-SCR, FTIR, XAS, XES, *in situ* spectroscopy

TEXT

The selective catalytic reduction with ammonia (NH_3-SCR) is an effective way to remove hazardous NO_x compounds from automotive gas emissions.[1-4] Among the various catalysts tested for this purpose, copper-containing zeolites showed high performance over a wide range of temperatures and conditions. In particular, due to its superior thermal stability, small pore Cu-SSZ-13 zeolite has been recently selected as a promising candidate for commercial applications.[1,5-7] During the last few years an impressive amount of papers appeared in literature aiming to clarify the catalytic cycle of the NH_3-SCR reaction over Cu-zeolites,[1-8] but up to now a clear picture is still missing.

Traditionally, on the base of previous study on vanadia catalyst,[2] two main NH_3-SCR mechanisms have been proposed over Cu-zeolites: in the Langmuir-Hinshelwood mechanism the interaction between adsorbed NH_3 and surface nitrite and nitrate is thought to be the key step of the reaction;[8,9] conversely, in the Eley-Rideal mechanism gas-phase NO_2 interacts with two adjacent NH_4^+ ions to form a $(NH_4)_xNO_2$ complex.[2] Both mechanisms are based on the fact that firstly NO needs to be oxidized to NO_2 (or directly converted to nitrate/nitrite species) which can be further reduced to N_2 and H_2O.[2] Recently, Gao *et al.*[1] proposed a new low temperature mechanism where they claim the importance of the NH_3–Cu^+–NO^+ complex formation as an alternative way to the initial NO oxidation step. Contextually, Ruggeri *et al.* stated that the oxidation of NO to NO_2 as rate determining step of the standard SCR reaction is remarkably questionable.[10] In all the reported mechanisms adsorbed NH_3 species play a crucial role since they act as reducing agent of NO. Hence, the study of the interaction between the catalyst and NH_3 is fundamental. FTIR spectroscopy is a powerful technique in catalysis,[11-13] which has been successfully employed to identify different kind of adsorbed ammonia species involved in the SCR catalytic cycle.[14-17] Commonly, two types of adsorbed NH_3 could be easily detected by infrared spectroscopy: *(i)* NH_3 coordinated to Lewis acid sites (Cu sites, extraframework Al^{3+}), with the formation of corresponding amino complexes which usually give rise to an absorption band at around 1620 cm^{-1} associated to δ_{as}(NH) mode (corresponding δ_s(NH) mode usually lies at frequencies lower than 1250 cm^{-1}, becoming overshadowed by the high intensity modes of the zeolitic structure); *(ii)* NH_3 interacting with residual bridged hydroxyls groups, *i.e.* Brønsted acid sites, with the formation of NH_4^+ ions and the appearance of corresponding signals in the 1500–1350 cm^{-1} range. In the latter case, the occurrence

of solvated NH_4^+ species, *i.e.* $NH_4^+ \cdot nNH_3$ ($n \geq 1$), is also possible, depending on temperature and NH_3 coverage.[18-20]

FTIR spectroscopy of adsorbed NH_3 is able to provide a comprehensive view on the different NH_3-adsorbed species, allowing their identification. However the technique lacks sensitivity in the electronic and geometric properties of the adsorbing site, which could be crucial to obtain further insights on the SCR mechanism. Conversely, direct information on the local coordination geometry and electronic properties of the Cu sites can be accessed by XAS and XES spectroscopies, exploiting the element selectivity of the techniques.[21-23] XAS has already been employed in the characterization of the Cu-SSZ-13 zeolite, to clarify the local coordination environment of the metal sites in the calcinated material[24] and to monitor its evolution in SCR-relevant conditions.[4,25,26] These studies related the high catalytic performance of Cu-SSZ-13 to the presence of isolated mononuclear Cu^{2+} species in the zeolite cavities. Indeed, the band at 22700 cm^{-1} (440 nm) in the UV-Vis and the Raman bands at 270, 455, 870 cm^{-1} (that undergo Raman enhancement when excited with the 488 nm laser), observed in Cu-ZSM-5,[27] are not present in this Cu-SSZ-13 sample.[28]

Due to the complexity of the interaction between the Cu centers and the reactants in SCR-conditions, it is difficult to unambiguously distinguish the role of each gas feed component in the reaction mechanism and to identify the principal intermediates species. Hence, it is important to separately investigate the interaction of each reactant with the catalyst. However, to the best of our knowledge, no previous XAS or XES studies focused on the adsorption of NH_3 on Cu-SSZ-13 have been reported in the literature, although they are indispensable to clarify the local atomic and electronic structure of the resulting species. Here we report a multi-technique investigation of the NH_3 interaction with the Cu-SSZ-13 catalyst, combining FTIR spectroscopy, sensitive to the different NH_3 adsorption sites in the zeolite, and XAS/XES methods, which provide selective information on the NH_3 coordination to the Cu sites relevant for the SCR reaction.

Prior to ammonia adsorption, the sample needs to be dehydrated; it is well known that dehydration process modifies the initial oxidation state of copper depending on the type of activation conditions. XANES measurements were performed to characterize the Cu-SSZ-13 samples activated *in vacuo* and in O_2/He flux in order to appreciate the differences in the oxidation state and the local coordination geometry of Cu centers. Figure 1 reports the XANES spectra of Cu-SSZ-13 in its hydrated state, collected at room temperature (blue curve), and after activation at 400 °C performed both in O_2/He flux (black curve) and *in vacuo* (green curve). The XANES spectrum of the hydrated Cu-SSZ-13 shows the typical features of hydrated Cu^{2+} ions,[29,30] in accordance with previous literature on Cu-zeolites prepared by aqueous ion exchange.[26,31-34]

In particular, a weak pre-edge peak **A** is clearly observed at ~ 8977.3 eV. This transition is conventionally assigned to *1s* → *3d* transition in Cu^{2+}.[35-38] However, a minor *1s* → *4p* contribution is also expected to be involved. In addition, for the hydrated sample, a high-intensity white line feature **D** is present at ~ 8995.3, typical of Cu^{2+} centers in a highly coordinated form, *e.g.* when the coordination sphere of the cation is saturated by water molecules or by a combination of framework oxygens, water molecules and, eventually, OH groups.[33]

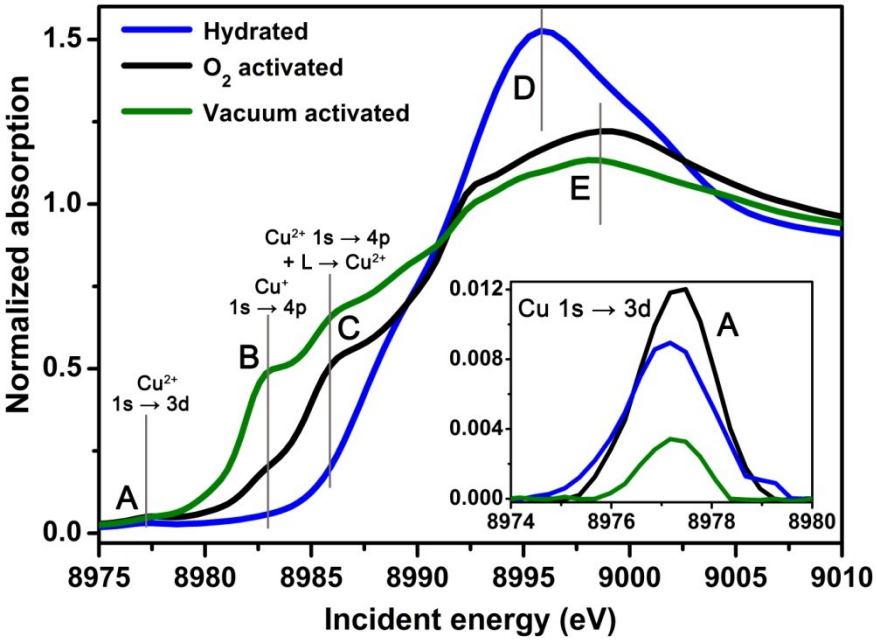

Figure 1. Cu K-edge XANES spectra of Cu-SSZ-13 in its hydrated state (blue curve) collected at room temperature, and after the activation process at 400 °C, performed both *in vacuo* conditions (green curve) and in O_2/He flux (black curve). The principal XANES features are labeled with the **A**–**E** letters, and the inset reports a magnification of the background-subtracted XANES spectra in the region where the weak Cu^{2+} *1s* → *3d* peak (**A**) is observed.

It is worth noting that the **A** transition is not present in Cu^+ complexes, due to their d^{10} configuration.[34] Thus, it can be employed to fingerprint the presence of Cu^{2+} and qualitatively evaluate its abundance in the investigated samples by examining the background subtracted intensity of the correspondent pre-edge peak. Nonetheless, it has been shown that the intensity and the shape of the **A** feature are also influenced by the symmetry of the local Cu^{2+} coordination environment and therefore by the level of *3d-4p* orbital mixing.[36,39] Hence, more reliable information on the Cu oxidation state is obtained by considering the intensity of peak **A** in conjunction with the other relevant XANES features.

Upon *in vacuo* heating from RT to 400 °C, a clear evolution of the XANES feature is observed. Finally, for *vacuum* activated Cu-SSZ-13 sample, the intensity of feature **A** is significantly reduced with respect to the hydrated sample, although a residual peak is still present. In addition, the white line resonance **D** shifts at higher energy (at ~ 8998.6 eV, peak **E**) and two main transitions appear in the pre-edge region: a distinct peak **B** at ~ 8982.8 eV and a shoulder **C** at ~ 8986.3 eV.

Interestingly, XANES spectra for Cu^+ systems are commonly characterized by distinct pre-edge features in the 8982–8985 eV range, whereas for the Cu^{2+} species pre-edge peaks below 8985 eV are mostly not observed,[35] except for the *1s* → *3d* transition previously discussed. According to this general trend, feature **B** is assigned the *1s* → *4p* transition of Cu^+.[35,40,41] The energy position of this feature, in the 8982–8984 eV range, is typical of two- or three-coordinated Cu^+ sites.[35,38] This assignment, in combination with the significant decrease in the intensity of feature **A**, strongly suggests that *vacuum* activation induces the "self reduction" of a substantial fraction of the initial Cu^{2+} sites to Cu^+, as previously reported *e.g.* for the Cu-ZSM-5 zeolite.[41,42]

Nevertheless, the reduction is not total, and a minor contribution from Cu^{2+} sites is still present, as demonstrated by the persistence of feature **A**. This was the case of Cu-MOR activated in the same conditions,[34] while a virtually total reduction to Cu^{+} was observed for Cu-ZSM-5.[42] This evidence is also supported by the presence of the shoulder **C,** assigned to the Cu^{2+} *1s* → *4p* + ligand (L) → Cu^{2+} charge transfer excitation,[43] similarly to what is observed in the planar $Cu(OH)_2$ complex[38] and already observed in activated Cu-SSZ-13.[25,26] It is however worth to note that a complete reduction of the Cu^{2+} centers could be reached by increasing the activation time, as was recently demonstrated by Giordanino *et al.*[28] using FTIR spectroscopy.

The overall shape of the XANES spectrum for the O_2-activated Cu-SSZ-13 is quite similar to that observed for *vacuum* activated sample, previously discussed. This analogy reflects the similarity in the local coordination environment of the Cu centers after the two different activation processes, resulting in oxygen-coordinated monomeric species isolated in the zeolite framework. However, two key-differences are observed, which point out significant variations in Cu oxidation state after O_2 and *vacuum* activation: (*i*) for the O_2-activated Cu-SSZ-13 a slight enhancement in the intensity of feature **A** with respect to the hydrated material is observed, as expected due to the lowering in Cu^{2+} coordination symmetry upon dehydration and increased interaction with the zeolite framework;[34,36,39,42] (*ii*) the pre-edge region for the O_2-activated sample is dominated by feature **C**, typical of Cu^{2+} centers, while the **B** peak, diagnostic for the Cu^{+} presence, is remarkably less intense with respect to the one found after *vacuum* activation.

These evidences demonstrate that the O_2-activation is effective in limiting the "self reduction" process[34,42] in Cu-SSZ-13, and results in a majority of Cu^{2+} sites, with a minor contribution from reduced Cu^{+} centers.

Since an oxidative activation reflects the real working condition of the catalyst,[44] hereinafter we mainly focus on the NH_3 adsorption on O_2-activated sample, which contains a majority of Cu^{2+} centers as follows from the XANES analysis.

Ammonia (PA = 853. 5 KJ mol^{-1}) is known as typical strong base.[45] The kinetic diameter of ammonia based on the Lennard-Jones relationship is 2.6 Å. Since the diameter of 8MR of the CHA structure is ~3.8 Å, an ammonia molecule reaches almost all acid sites, *i.e.* Lewis and Brønsted sites in zeolites.

Figure 2 shows the infrared spectra recorded on the O_2-activated sample during the exposure to ammonia at 100 °C. Starting from low ammonia coverage, a gradual consumption of the 3611 and 3584 cm^{-1} bands related to ν(OH) of bridged hydroxyls with a strong Brønsted acidity[46] is observed.

It is worth to note that, as also previously observed by Lezcano-Gonzalez et al.,[17] the intensity of the bands related to ν(OH) modes of Brønsted sites is surprisingly high and quite comparable with the parent material H-SSZ-13. This is an interesting evidence, because the intensity of these bands should decrease consistently in a sample characterized by a Cu/Al ratio of 0.444. In particular, it is commonly assumed that, when copper is introduced in the zeolitic framework upon aqueous ion exchange, the positive charge (+2) of Cu^{2+} ions must be balanced by two negative charges, likely represented by two aluminum atoms in close proximity. Therefore, a ratio of Cu/Al = 0.5 should represent the total ion exchange level. Conversely, our results clearly show that a consistent concentration of not exchanged sites, *i.e.* Brønsted sites, is still present even if the Cu/Al ratio is not far from the stoichiometric exchange level. This is a novel evidence which suggests that likely, during the exchange procedure, part of Brønsted sites are exchanged by monovalent copper

complexes, such as $[CuOH]^+$.[28] Further studies would be required to clarify this point, possibly allowing to revisit the nature of the Cu sites in the activated catalyst.

The FTIR bands related to ν(OH) of bridged hydroxyls with a strong Brønsted acidity totally disappear when $NH_3/H^+ = 1$ (green curve). Simultaneously, complex absorption features develop in the 1550–1350 cm^{-1} region, showing two main component at 1456 and 1380 cm^{-1} which shift to higher wavenumbers for $NH_3/H^+ > 1$, together with the appearance of new features in the 3400–3100 cm^{-1} range. These bands are commonly associated to the δ(NH) and ν(NH) modes, respectively, of NH_4^+ ion formed upon NH_3 protonation by Brønsted acidic hydroxyls groups.[18] Concurrently to the formation of NH_4^+ ions, the interaction of NH_3 with Lewis copper sites is confirmed by the appearance of the band at 1624 cm^{-1}.[14] It is important to note that also the presence of extra-framework Al (EFAl) could give a contribution at the same frequency.[17] This band was not observed on H-SSZ-13 zeolite activated in the same conditions of Cu-SSZ-13 (see Supporting Information, Figure S1); in addition, ^{27}Al MAS SSNMR spectrum of H-SSZ-13 (see Supporting Information, Figure S4) reveals a concentration of octahedral-like Al species lower than 5%, excluding the presence of a significant fraction of EFAl species in the samples under investigation. Moreover, the 1624 cm^{-1} band could be associated to molecular ammonia bounded on both Cu^+ and Cu^{2+} sites; indeed, the band does not change in intensity and position if ammonia is dosed on both *vacuum* and O_2-activated samples (see Supporting Information, Figure S2) where a prevalence of Cu^+ and Cu^{2+} centers is expected, respectively.[28]

The fact that 1550–1350 cm^{-1} and 1624 cm^{-1} features develop together suggests similar adsorption energy of the two acidic sites. A gradual but not total consumption of 3737 cm^{-1} band is also observed, due to the interaction of ammonia with the silanols prevalently located on external surfaces of the catalyst. Additionally, the band at 3656 cm^{-1} that we recently associated to $[Cu^{2+}OH^-]^+$ sites[28] is also eroded, indicating that ammonia could be adsorbed even on these particular sites. It is worth noting that this band is consumed only after the saturation of all Brønsted sites ($NH_3/H^+ = 1$).

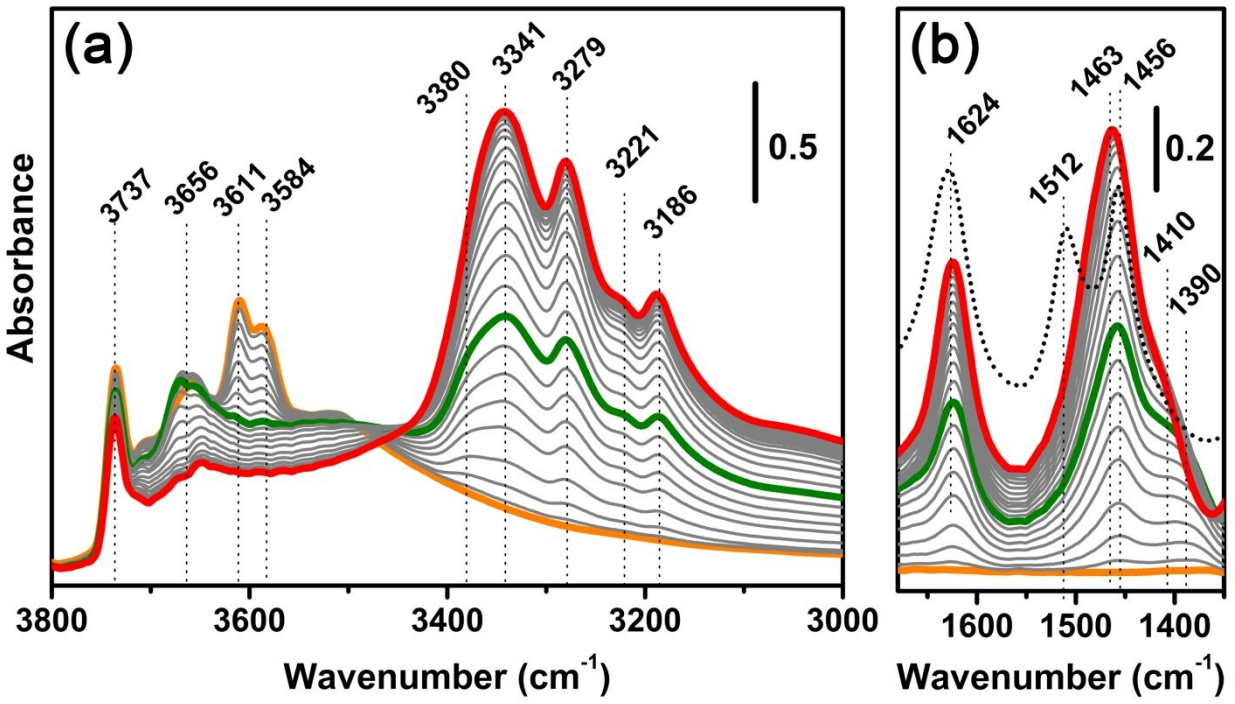

Figure 2. FTIR spectra of Cu-SSZ-13 at increasing contact time with 1800 ppm of NH_3/He mixture (100 °C). Spectra are reported in both ν(NH) (panel (a)) and δ(NH) (panel (b), spectra reported after the subtraction of the spectrum of the dehydrated zeolite sample) regions. Orange curve refers to activated sample, red curve refers to highest contact time, *i.e*, highest ammonia loading, grey curves relate to intermediate ammonia loadings. Green curve refers to the total consumption of Brønsted sites. Dotted black curve in panel (b) refers to the spectrum of Cu-SSZ-13 upon NH_3 adsorption at room temperature.

The nature of ammonia complexes in H-form zeolites has been studied by Zecchina *et al.*[18] The authors revealed that, at room temperature, in H-ZSM-5, H-BEA, HY and H-SAPO-34, framework oxygens stabilize mostly bidentate and tridentate ammonium ions. In particular, the triple degeneracy of the ν_4 mode of the "free" NH_4 ions (T_d symmetry) is removed due to the H-bonding, leading to an absorption feature in the 1550–1350 cm^{-1} region. Since the frequency of these bands can change depending on symmetry or different adsorption sites, it can be expected that ν_4 bands of the NH_4^+ ions appear as a featureless and broad band. As reported in Figure 3c, the deconvoluted spectrum of the NH_4^+ ions recorded at 100 °C shows three main components at 1463, 1456 and 1406 cm^{-1}. Lónyi *et al.*[20] observed similar bands dosing NH_3 on acidic porous materials. The authors stressed the fact that the component bands resolved in the 1550–1300 cm^{-1} region cannot be assigned to the ν_4 modes of a single H-bounded NH_4^+ species, but to overlapping bands of NH_4^+ ions H-bounded to various extent in $NH_4^+ \cdot n NH_3$ associations ($n \geq 1$). Indeed, it is expected that for $NH_4^+ / H^+ > 1$ the coordination of ammonia to NH_4^+ ions leads the formation of $NH_4^+ \cdot n NH_3$ species. In particular, it has been observed that H-bonding of NH_3 to the zeolite-bounded NH_4^+ ions shifts the ν_4 bands of the ion at higher wavenumbers of an extent likely dependent on the number of NH_3 molecules, *i.e. n* value, which solvate the NH_4^+ ions[20] With this respect, the last statement is supported by the appearance of the highly blue shifted band at 1512 cm^{-1} (dotted black curve in Figure 2b) that we observe after adsorption of high partial pressures of NH_3 at room temperature. A similar band was observed by other authors, [20,47] and it has been associated to a bending vibration of NH_4^+ species H-bounded to NH_3. The absence of the well resolved band at 1512 cm^{-1} in the other spectra reported in Figure 2b does not exclude the occurrence of $NH_4^+ \cdot n NH_3$ associations at 100°C. Indeed, spectra collected at this temperature are characterized by bands at 1700 and 2770 cm^{-1} (see supporting information, Figure S3) which have been assigned to bending mode of molecular ammonia coordinated to NH_4^+ ions and to N-H stretching mode of NH_4^+ ions H-bounded to NH_3. [18,48]

The changes in the infrared spectra recorded during the NH_3 desorption process (Figure 3) allowed us to study the thermal stability of different ammonia species and better investigate the complex band contributions due to $NH_4^+ \cdot n NH_3$ associations in the 100-500°C temperature range. In the bending region (Figure 3b) the desorption process is accompanied by a gradual intensity decrease of the band at 1624 cm^{-1}, which totally disappear at 500 °C indicating that at this temperature ammonia bounded to copper sites is completely desorbed. Conversely, the complex signal related to protonated ammonia is still persistent at 500 °C, suggesting a high thermal stability of these species with comparison to NH_3 bounded on copper sites. This is likely related to the stabilization of the NH_4^+ ions via H-bonding to the framework oxygens. Starting from 100 °C, the evolution of the NH_4^+ signal during the desorption process could be ascribed as follows: the

intensity decrease and the red shift of the component at 1463 cm^{-1} is accompanied in the 100–400 °C temperature range by the growth in intensity of the component at around 1400 cm^{-1}, which evolves at high temperature in a unique broad band centred at 1430 cm^{-1}; this behaviour clearly indicates that during the desorption process the species associated with the band at 1463 cm^{-1} are transformed into the species related to the 1430 cm-1 band.. This is supported by the observed isosbestic point at 1440 cm^{-1}. Taking in account that the solvation effect shifts the vibration modes of NH_4^+ ions to higher wavenumbers as evidenced by the appearance at room temperature of the band at 1512 cm^{-1} (see Figure 2b), the band at 1463 cm^{-1} could be still considered a manifestation of $NH_4^+ \cdot nNH_3$ associations. It is however important to note that at 100°C, *n* value is likely lower than room temperature, due to the fact that an increased temperature could limit the amount of solvating NH_3 molecules. Deconvoluted spectra[49] at different desorption temperature (Figure 3c) show that the 1430 cm^{-1} band is composed by two main components at 1450 and 1400 cm^{-1} which rise in intensity at the expense of the band at 1463 cm^{-1}: these two bands could be easily assigned to the anti-symmetric and symmetric bending vibrations of not solvated NH_4^+ ions, respectively.[17] In the 400–500 °C temperature range the 1430 cm^{-1} band decreases in intensity, while the intensity of the signals at 3611 and 3584 cm^{-1} is partially restored; contemporaneously, the bands in the 3400–3100 cm^{-1} range decrease in intensity, shifting to higher wavenumbers at high temperature (Figure 3a). On the base of these observations one can conclude that the desorption of solvating ammonia molecules from $NH_4^+ \cdot nNH_3$ associations (likely represented by the band at 1463 cm^{-1}) leads to not solvated NH_4^+ ions (characterized by deconvoluted components at ν_{as} = 1450 cm^{-1} and ν_s = 1430 cm^{-1}), which can further decompose for T > 400 °C as follow: $NH_4^+ \rightarrow NH_3 + H^+$.

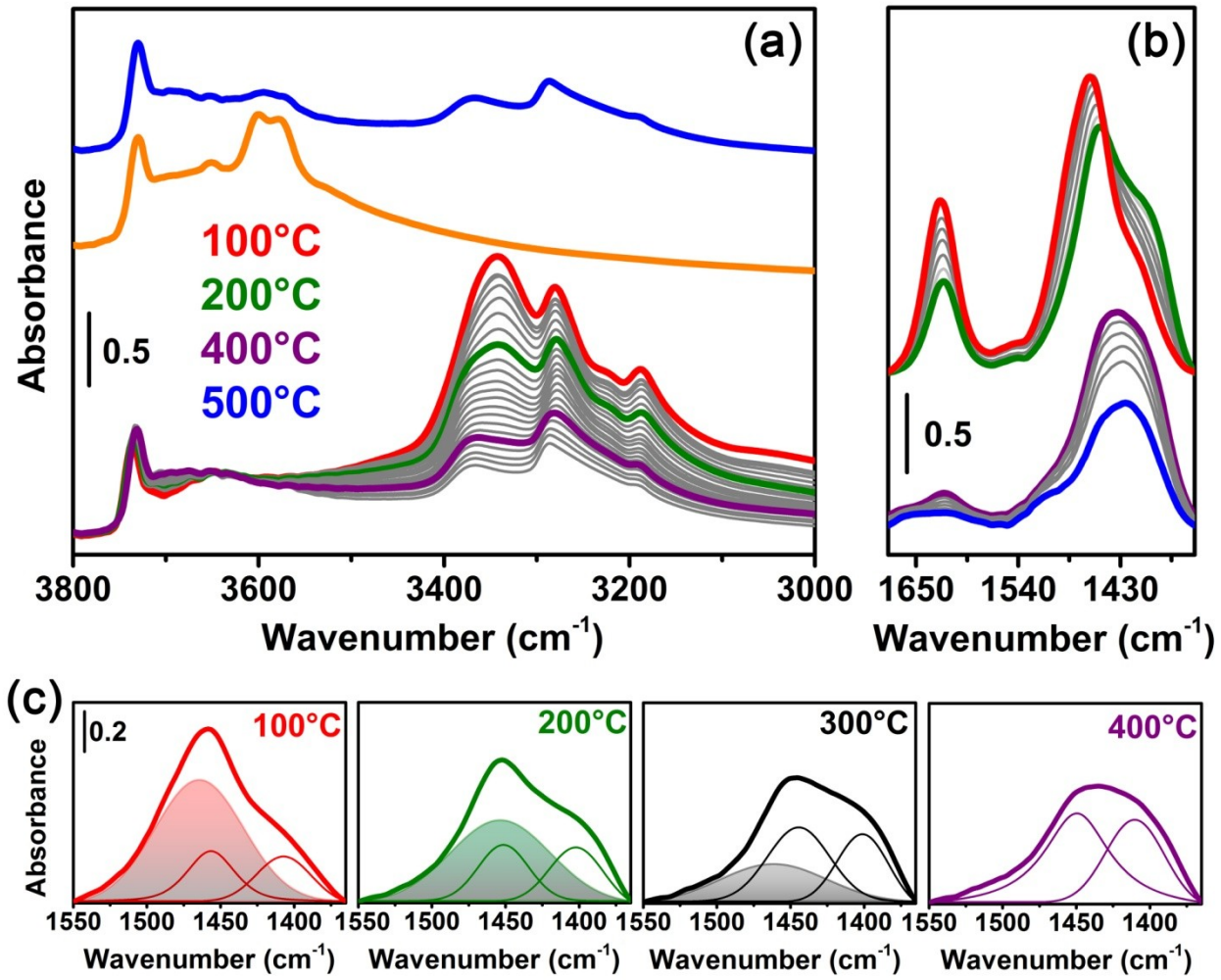

Figure 3. Helium NH_3-temperature programmed desorption (TPD) over Cu-SSZ-13 followed by FTIR in the 100–500 °C temperature range. Spectra are reported in both ν(NH) (panel (a)) and δ(NH) (panel (b), spectra reported after the subtraction of the spectrum of the dehydrated zeolite sample) regions. Grey curves refer to spectra recorded at intermediate temperature. In panel (a), the spectrum of dehydrated sample is also reported (orange curve). Panel (c) shows the deconvoluted δ(NH) spectra of NH_4^+ ions at different desorption temperature. Filled area refers to $NH_4{\cdot}nNH_3$ associations band observed at 1460 cm^{-1}. The two other components at 1450 and 1400 cm^{-1} refer to the anti-symmetric and symmetric bending vibrations of NH_4^+.

Summarizing, from FTIR analysis we identified different kind of adsorbed ammonia potentially available for SCR reaction: *(i)* NH_3 bounded to copper sites, *i.e.* both isolated Cu^{2+} and $[Cu^{2+}OH^-]^+$ sites; *(ii)* protonated NH_3 as NH_4^+ ionic form, *i.e.* NH_3 bounded to Brønsted sites; *(iii)* solvated NH_4^+ ions, *i.e.* $NH_4^+{\cdot}nNH_3$ associations. Species *(i)* and *(iii)* have been found to be more stable for T < 400 °C, while at higher temperature species *(ii)* is the more abundant.

Interaction of Cu-SSZ-13 with NH_3 was also monitored *in situ* by $K\beta_{1,3}$ HERFD (high energy resolution fluorescence detection) XANES (Figure 4a). Initial spectrum corresponds to the sample activated at 400 °C in oxygen/helium flux and is equivalent to the one presented in Figure 1. The only difference is that the pre-edge peaks are more pronounced compared to conventional XANES because of the lower level of background.[22,23,50] The high intensity of the pre-edge *1s* → *3d*

transition **A** confirms that the copper oxidation state is close to +2. However, when ammonia is introduced in the reactor, the area of this pre-edge feature starts to decrease steadily and reaches the minimum of around 10% of its initial value in the NH_3-saturated state at end of the adsorption process (see the inset of Figure 4a). At the same time the peak **B** at 8982.5 eV, which is characteristic for Cu^+ species,[35] rises dramatically surpassing even the main edge maximum. This serves as a clear indication for the reduction of Cu species from Cu^{2+} to Cu^+. Moreover, such a high intensity of the peak **B** suggests a linear coordination of the Cu species.[35,51,52] In the adopted experimental conditions, this could be either a O_{fw}–Cu–NH_3 configuration, where copper is still coordinated to one framework oxygen O_{fw}, and/or the H_3N–Cu–NH_3 structure, where copper forms a complex with the two NH_3 molecules inside the zeolite cavity. Similar complex has already been reported in a zeolitic framework (ferrierite) and well characterized by X-ray diffraction, as described in the study of Gomez-Lor et al.[53] In that case the distances between copper and the nearest oxygen were 3.95 Å. The formation of a O_{fw}–Cu–O_{fw} linear species can be ruled out since the NH_3 coordination to copper is clearly evidenced by Cu X-ray emission spectra (Figure 4b). Firstly, the significant alteration of the $K\beta_{2,5}$ line shape indicates the different local coordination geometry and symmetry at the initial and final stages of the adsorption process, as previously observed on Ti silicalite-1 (TS-1) upon NH_3 adsorption.[54,55] Secondly, the blue-shift of the Kβ'' satellite for the final product with respect to the initial stage with oxygen-only coordination proves the formation of Cu–N bond. Indeed, this peak originates from the ligand *2s* to metal *1s* cross-over transition and is therefore sensitive to the binding energy of the ligand *2s* orbital.[56,57] Since the nitrogen *2s* level lies higher in energy than the one of oxygen, the coordination of the former causes the blue-shift of the peak.

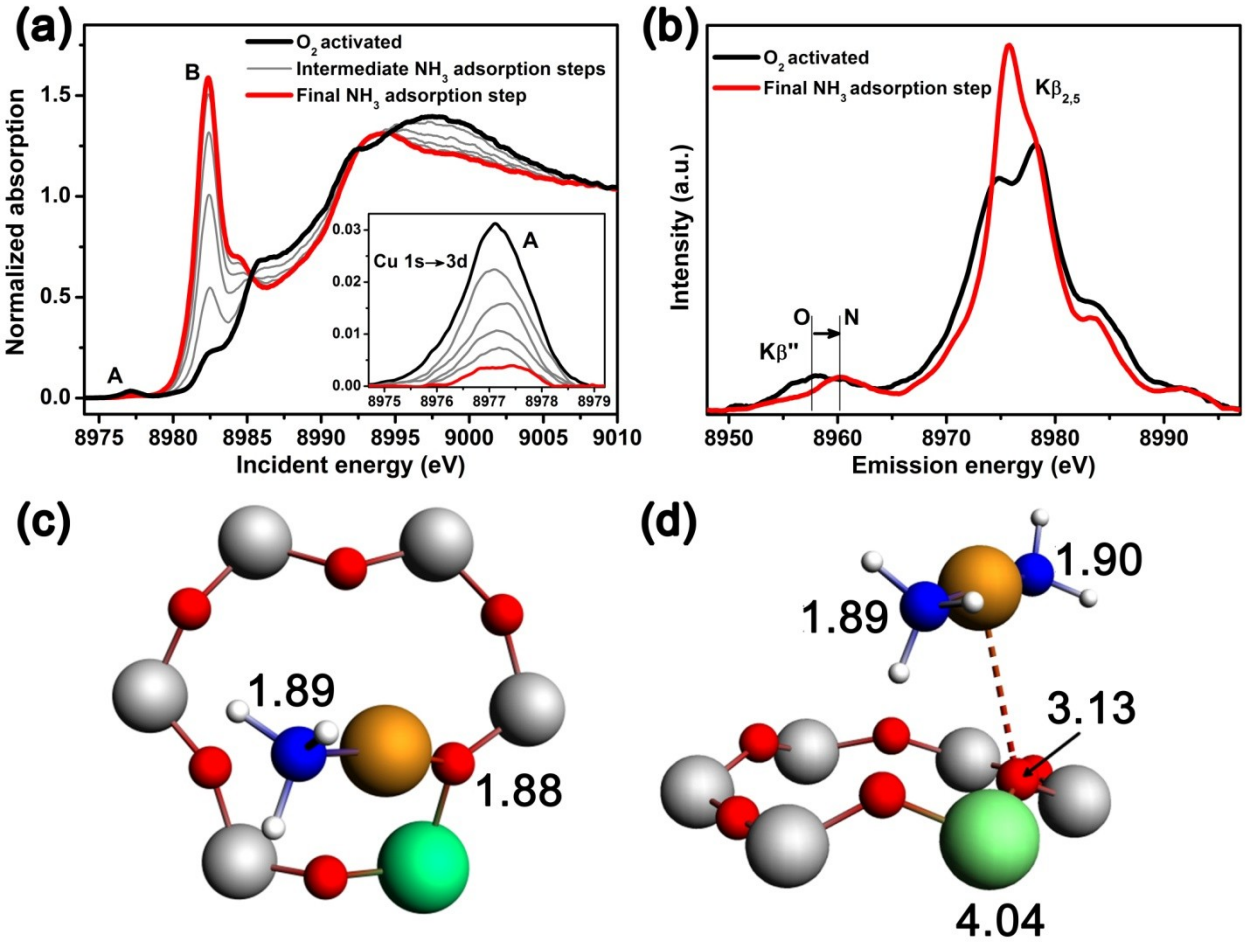

Figure 4. (a) *In-situ* evolution of the Cu K-edge HERFD XANES spectra of O_2/He-activated Cu-SSZ-13 during the interaction with a flow of 1300 ppm NH_3 in He at 120 °C. The inset magnifies the pre-edge region with the background subtracted. (b) Background-subtracted Cu $K\beta_{2,5}$ and Kβ'' emission lines for the initial and final stages of the process. (c) and (d) Cu local environment after adsorption of one and two NH_3 molecules, respectively (only the 6-ring atoms are shown). Color code: orange – Cu, green – Al, grey – Si, red – O, blue – N, white – H. Distances between Cu and neighboring atoms are indicated in Å.

In order to support these structural findings, DFT calculations were carried out using ADF2012 package.[58,59] Geometry optimization was performed adding NH_3 molecules in the vicinity of the Cu atom placed in the d6r on the base of the previous work by Deka et al.[25] Results indicate that a single NH_3 ligand drives Cu ion outside of the d6r plane forming an almost linear O_{fw}-Cu-NH_3 structure with O-Cu-N angle of 172° (Figure 4c). The second ammonia molecule lifts Cu even higher in the large cavity while the N-Cu-N angle reaches 177° (Figure 4d). Both structures are in agreement with the XANES and XES data discussed above. However, due to the similarity of bond distances and angles, discrimination between these two possible cases remains an ongoing challenge.

The reduction of a transition metal centre M due to NH_3 dissociative chemisorption, reaction (a), has been already proposed for oxide-based materials employed as ammonia oxidation catalysts.[60]

The process involves the activation of ammonia, possibly via the amide species, which is followed by a coupling reaction that yields nitrogen as ammonia oxidation product, reaction (b):

$$NH_3 + M^{n+} + O^{2-} \rightarrow M^{(n-1)+}{-}NH_2 + {}^{-}OH \qquad (a)$$

$$2\ M^{(n-1)+}{-}NH_2 \rightarrow N_2H_4 \rightarrow N_2 + 4H^+ + 4e^- \qquad (b)$$

Cu-zeolites typically show a good ammonia oxidation activity at relative high temperature.[61] However, in our case, reaction (b) is supposed to be unfovoured because it is improbable to find two metal centers close enough to allow the formation of N_2H_4. This is particularly true for Cu-SSZ-13 catalyst which has been claimed to contain mainly well dispersed isolated copper ions. Although reaction (a) is still compatible with our XAS/XES results, it is in contrast with FTIR analysis. Indeed, the formation of $–NH_2$ like groups should give rise to absorption features at around 3520, 3440 and 1550-1510 cm^{-1}, associated with ν(NH) and δ(NH) modes, respectively,[62-66] which are not observed in our spectra collected at 100°C (see Figure 2). On the base of these observations, a dissociative chemisorption of NH_3 on copper sites is unlikely, while a simple molecular coordination remains the most probable scenario. In order to explain the reduction of copper sites and their capability to form linear complexes as clearly demostrated by XAS/XES, an alternative pathway needs to be proposed:

$$Cu^{2+} + e^- \rightarrow Cu^+ \qquad (c)$$

$$2NH_3 \rightarrow 6H^+ + 6e^- + N_2 \qquad (d)$$

In this case NH_3 oxidation, reaction (d), represents the electron supply needed for the reduction of Cu^{2+}sites, reaction (c). In turn, Cu^+ ions could coordinate one or two NH_3 molecules leading to the formation of linear complexes. Despite this mechanism needs to be supported by further experimental evidences, the Cu reduction observed by HERFD-XANES concomitantly to NH_3 adsorption (Figure 4) has potential implications on revisiting the low-temperature SCR mechanism. Indeed, these evidence highlights that coordinated NO is not the only SCR reactant able to reduce Cu^{2+},[1,67] and that a key role in the Cu^{2+}/Cu^+ redox cycle could be also played by ammonia. In addition, the observed possibility to stabilize a Cu(I) complex inside SSZ-13 zeolitic matrix could open new synthetic routes for the preparation of novel Cu-based catalyst starting from Cu(I) precursors. So far, a totally-exchanged Cu zeolite system has been prepared starting from CuCl gas phase ion exchange,[32] a way which does not guarantee the absence of chloride-like extra phases[68] with compromising effects on the catalytic activity of the final material. Conversely, the use of a chloride-"free" precursor, *i.e.* Cu(I)-amino complex, could results in a enhanced purity and consequently improved performance.

ASSOCIATED CONTENT

Supporting Information.

Additional FTIR spectra, ^{27}Al MAS NMR analysis and experimental/computational details are reported.

This material is available free of charge via the Internet at http://pubs.acs.org

AUTHOR INFORMATION

Corresponding Author

*Email: silvia.bordiga@unito.it

ACKNOWLEDGMENTS

This work has been supported by "Progetti di Ricerca di Ateneo-Compagnia di San Paolo-2011-Linea 1", ORTO11RRT5 project. CL, KAL and AVS thank the support from the Mega-grant of the Russian Federation Government to support scientific research at Southern Federal University, No.14.Y26.31.0001. The authors would like to acknowledge P. Glatzel, C. Lapras and O. Mathon for their help during beamtime at the ID26 and BM23 beamlines, ESRF. We are also grateful to A. P. Molina for her contribution and valuable discussions during experiments performed at the ID26 beamline (ESRF) and to M. R. Chierotti and R. Gobetto for having performed ^{27}Al MAS NMR measurements.

REFERENCES

(1) Gao, F.; Kwak, J.; Szanyi, J.; Peden, C. F. Current Understanding of Cu-Exchanged Chabazite Molecular Sieves for Use as Commercial Diesel Engine DeNO$_x$ Catalysts. *Top. Catal.* **2013,** *56*, 1441-1459.

(2) Brandenberger, S.; Krocher, O.; Tissler, A.; Althoff, R. The State of the Art in Selective Catalytic Reduction of NO$_x$ by Ammonia Using Metal-Exchanged Zeolite Catalysts. *Catal. Rev.* **2008,** *50*, 492-531.

(3) Gabrielsson, P. L. T. Urea-SCR in Automotive Applications. *Top. Catal.* **2004,** *28*, 177-184.

(4) Deka, U.; Lezcano-Gonzalez, I.; Weckhuysen, B. M.; Beale, A. M. Local Environment and Nature of Cu Active Sites in Zeolite-Based Catalysts for the Selective Catalytic Reduction of NO$_x$. *ACS Catal.* **2013,** *3*, 413-427.

(5) Fickel, D. W.; D'Addio, E.; Lauterbach, J. A.; Lobo, R. F. The Ammonia Selective Catalytic Reduction Activity of Copper-Exchanged Small-Pore Zeolites. *Appl. Catal. B-Environ.* **2011,** *102*, 441-448.

(6) Fickel, D. W.; Fedeyko, J. M.; Lobo, R. F. Copper Coordination in Cu-SSZ-13 and Cu-SSZ-16 Investigated by Variable-Temperature XRD. *J. Phys. Chem. C* **2010,** *114*, 1633-1640.

(7) Kwak, J. H.; Tonkyn, R. G.; Kim, D. H.; Szanyi, J.; Peden, C. H. F. Excellent Activity and Selectivity of Cu-SSZ-13 in the Selective Catalytic Reduction of NO$_x$ with NH$_3$. *J. Catal.* **2010,** *275*, 187-190.

(8) Grossale, A.; Nova, I.; Tronconi, E.; Chatterjee, D.; Weibel, M. NH_3-NO/NO_2 SCR for Diesel Exhausts Aftertreatment: Reactivity, Mechanism and Kinetic Modelling of Commercial Fe- and Cu-Promoted Zeolite Catalysts. *Top. Catal.* **2009,** *52*, 1837-1841.

(9) Ruggeri, M. P.; Grossale, A.; Nova, I.; Tronconi, E.; Jirglova, H.; Sobalik, Z. FTIR in Situ Mechanistic Study of the NH_3-NO/NO_2 Fast SCR Reaction over a Commercial Fe-ZSM-5 Catalyst. *Catal. Today* **2012,** *184*, 107-114.

(10) Ruggeri, M.; Nova, I.; Tronconi, E. Experimental Study of the NO Oxidation to NO_2 over Metal Promoted Zeolites Aimed at the Identification of the Standard SCR Rate Determining Step. *Top. Catal.* **2013,** *56*, 109-113.

(11) Lamberti, C.; Groppo, E.; Spoto, G.; Bordiga, S.; Zecchina, A. Infrared Spectroscopy of Surface Transient Species. *Adv. Catal.* **2007,** *51*, 1-74.

(12) Lamberti, C.; Zecchina, A.; Groppo, E.; Bordiga, S. Probing the Surfaces of Heterogeneous Catalysts by in Situ IR Spectroscopy. *Chem. Soc. Rev.* **2010,** *39*, 4951-5001.

(13) Vimont, A.; Thibault-Starzyk, F.; Daturi, M. Analysing and Understanding the Active Site by IR Spectroscopy. *Chem. Soc. Rev.* **2010,** *39*, 4928-4950.

(14) Zhu, H.; Kwak, J. H.; Peden, C. H. F.; Szanyi, J. In Situ DRIFT-MS Studies on the Oxidation of Adsorbed NH_3 by NO_x over a Cu-SSZ-13 Zeolite. *Catal. Today* **2013,** *205*, 16-23.

(15) Wang, D.; Zhang, L.; Kamasamudram, K.; Epling, W. S. In Situ-DRIFTS Study of Selective Catalytic Reduction of NO_x by NH_3 over Cu-Exchanged SAPO-34. *ACS Catal.* **2013,** *3*, 871-881.

(16) Sjövall, H.; Fridell, E.; Blint, R. J.; Olsson, L. Identification of Adsorbed Species on Cu-ZSM-5 under NH_3 SCR Conditions. *Top. Catal.* **2007,** *42*, 113-117.

(17) Lezcano-Gonzalez, I.; Deka, U.; Arstad, B.; Van Yperen-De Deyne, A.; Hemelsoet, K.; Waroquier, M.; Van Speybroeck, V.; Weckhuysen, B. M.; Beale, A. M. Determining the Storage, Availability and Reactivity of NH_3 within Cu-Chabazite-Based Ammonia Selective Catalytic Reduction Systems. *Phys. Chem. Chem. Phys.* **2014,** *16*, 1639-1650.

(18) Zecchina, A.; Marchese, L.; Bordiga, S.; Paze, C.; Gianotti, E. Vibrational Spectroscopy of NH_4^+ Ions in Zeolitic Materials: An IR Study. *J. Phys. Chem. B* **1997,** *101*, 10128-10135.

(19) Datka, J.; Gora-Marek, K. IR Studies of the Formation of Ammonia Dimers in Zeolites TON. *Catal. Today* **2006,** *114*, 205-210.

(20) Lonyi, F.; Valyon, J. On the Interpretation of the NH_3-TPD Patterns of H-ZSM-5 and H-Mordenite. *Micr. Mesop. Mater.* **2001,** *47*, 293-301.

(21) Bordiga, S.; Groppo, E.; Agostini, G.; van Bokhoven, J. A.; Lamberti, C. Reactivity of Surface Species in Heterogeneous Catalysts Probed by in Situ X-Ray Absorption Techniques. *Chem. Rev.* **2013,** *113*, 1736-1850.

(22) Mino, L.; Agostini, G.; Borfecchia, E.; Gianolio, D.; Piovano, A.; Gallo, E.; Lamberti, C. Low-Dimensional Systems Investigated by X-Ray Absorption Spectroscopy: A Selection of 2d, 1d and 0d Cases. *J. Phys. D-Appl. Phys.* **2013,** *46*, 423001.

(23) Singh, J.; Lamberti, C.; van Bokhoven, J. A. Advanced X-Ray Absorption and Emission Spectroscopy: In Situ Catalytic Studies. *Chem. Soc. Rev.* **2010,** *39*, 4754-4766.

(24) Korhonen, S. T.; Fickel, D. W.; Lobo, R. F.; Weckhuysen, B. M.; Beale, A. M. Isolated Cu^{2+} Ions: Active Sites for Selective Catalytic Reduction of NO. *Chem. Comm.* **2011,** *47*, 800-802.

(25) Deka, U.; Juhin, A.; Eilertsen, E. A.; Emerich, H.; Green, M. A.; Korhonen, S. T.; Weckhuysen, B. M.; Beale, A. M. Confirmation of Isolated Cu^{2+} Ions in SSZ-13 Zeolite as Active Sites in NH_3-Selective Catalytic Reduction. *J. Phys. Chem. C* **2012,** *116*, 4809-4818.

(26) McEwen, J. S.; Anggara, T.; Schneider, W. F.; Kispersky, V. F.; Miller, J. T.; Delgass, W. N.; Ribeiro, F. H. Integrated Operando X-Ray Absorption and DFT Characterization of Cu-SSZ-13 Exchange Sites During the Selective Catalytic Reduction of NO_x with NH_3. *Catal. Today* **2012,** *184*, 129-144.

(27) Woertink, J. S.; Smeets, P. J.; Groothaert, M. H.; Vance, M. A.; Sels, B. F.; Schoonheydt, R. A.; Solomon, E. I. A $[Cu_2O]^{2+}$ Core in Cu-ZSM-5, the Active Site in the Oxidation of Methane to Methanol. *P. Natl. Acad. Sci. USA.* **2009,** *106*, 18908-18913.

(28) Giordanino, F.; Vennestrom, P. N. R.; Lundegaard, L. F.; Stappen, F. N.; Mossin, S. L.; Beato, P.; Bordiga, S.; Lamberti, C. Characterization of Cu-Exchanged SSZ-13: A Compared FTIR, UV-Vis and EPR Study with Cu-ZSM-5 and Cu-β with Similar Si/Al and Cu/Al Ratios. *Dalton Trans.* **2013,** *42*, 12741-12761.

(29) Salmon, P. S.; Neilson, G. W.; Enderby, J. E. The Structure of Cu^{2+} Aqueous-Solutions. *J. Phys. C.* **1988,** *21*, 1335-1349.

(30) Benfatto, M.; D'Angelo, P.; Della Longa, S.; Pavel, N. V. Evidence of Distorted Fivefold Coordination of the Cu^{2+} Aqua Ion from an X-Ray-Absorption Spectroscopy Quantitative Analysis. *Phys. Rev. B* **2002,** *65*, 174205.

(31) Larsen, S. C.; Aylor, A.; Bell, A. T.; Reimer, J. A. Electron Paramagnetic Resonance Studies of Copper Ion-Exchanged ZSM-5. *J. Phys. Chem.* **1994,** *98*, 11533-11540.

(32) Palomino, G. T.; Bordiga, S.; Zecchina, A.; Marra, G. L.; Lamberti, C. XRD, XAS, and IR Characterization of Copper-Exchanged Y Zeolite. *J. Phys. Chem. B* **2000,** *104*, 8641-8651.

(33) Alayon, E. M. C.; Nachtegaal, M.; Bodi, A.; van Bokhoven, J. A. Reaction Conditions of Methane-to-Methanol Conversion Affect the Structure of Active Copper Sites. *ACS Catal.* **2014,** *4*, 16-22.

(34) Llabrés i Xamena, F. X.; Fisicaro, P.; Berlier, G.; Zecchina, A.; Palomino, G. T.; Prestipino, C.; Bordiga, S.; Giamello, E.; Lamberti, C. Thermal Reduction of Cu^{2+} Mordenite and Re-Oxidation Upon Interaction with H_2O, O_2, and NO. *J. Phys. Chem. B* **2003,** *107*, 7036-7044.

(35) Kau, L. S.; Spirasolomon, D. J.; Pennerhahn, J. E.; Hodgson, K. O.; Solomon, E. I. X-Ray Absorption-Edge Determination of the Oxidation-State and Coordination-Number of Copper - Application to the Type-3 Site in Rhus-Vernicifera Laccase and Its Reaction with Oxygen. *J. Am. Chem. Soc.* **1987,** *109*, 6433-6442.

(36) Sano, M.; Komorita, S.; Yamatera, H. Xanes Spectra of Copper(II) Complexes - Correlation of the Intensity of the 1s-3d Transition and the Shape of the Complex. *Inorg. Chem.* **1992,** *31*, 459-463.

(37) Lamberti, C.; Bordiga, S.; Salvalaggio, M.; Spoto, G.; Zecchina, A.; Geobaldo, F.; Vlaic, G.; Bellatreccia, M. XAFS, IR, and UV-Vis Study of the Cu-I Environment in Cu-I-ZSM-5. *J. Phys. Chem. B* **1997,** *101*, 344-360.

(38) Groothaert, M. H.; van Bokhoven, J. A.; Battiston, A. A.; Weckhuysen, B. M.; Schoonheydt, R. A. Bis (μ–Oxo) Dicopper in Cu-ZSM-5 and Its Role in the Decomposition of NO: A Combined in Situ XAFS, UV-Vis-near-IR, and Kinetic Study. *J. Am. Chem. Soc.* **2003,** *125*, 7629-7640.

(39) Kervinen, K.; Bruijnincx, P. C. A.; Beale, A. M.; Mesu, J. G.; van Koten, G.; Gebbink, R.; Weckhuysen, B. M. Zeolite Framework Stabilized Copper Complex Inspired by the 2-His-1-Carboxylate Facial Triad Motif Yielding Oxidation Catalysts. *J. Am. Chem. Soc.* **2006,** *128*, 3208-3217.

(40) Tranquada, J. M.; Heald, S. M.; Moodenbaugh, A. R. X-Ray-Absorption near-Edge-Structure Study of $La_{2-X}(Ba,Sr)_XCuO_{4-Y}$ Superconductors. *Phys. Rev. B* **1987,** *36*, 5263-5274.

(41) Prestipino, C.; Berlier, G.; Xamena, F.; Spoto, G.; Bordiga, S.; Zecchina, A.; Palomino, G. T.; Yamamoto, T.; Lamberti, C. An in Situ Temperature Dependent IR, EPR and High Resolution Xanes Study on the NO/Cu^+-ZSM-5 Interaction. *Chem. Phys. Lett.* **2002,** *363*, 389-396.

(42) Palomino, G. T.; Fisicaro, P.; Bordiga, S.; Zecchina, A.; Giamello, E.; Lamberti, C. Oxidation States of Copper Ions in ZSM-5 Zeolites. A Multitechnique Investigation. *J. Phys. Chem. B* **2000,** *104*, 4064-4073.

(43) Kau, L. S.; Hodgson, K. O.; Solomon, E. I. X-Ray Absorption Edge and EXAFS Study of the Copper Sites in Zinc Oxide Methanol Synthesis Catalysts. *J. Am. Chem. Soc.* **1989,** *111*, 7103-7109.

(44) Koebel, M.; Elsener, M.; Kleemann, M. Urea-SCR: A Promising Technique to Reduce NO_x Emissions from Automotive Diesel Engines. *Catal. Today* **2000,** *59*, 335-345.

(45) Pazé, C.; Bordiga, S.; Lamberti, C.; Salvalaggio, M.; Zecchina, A.; Bellussi, G. Acidic Properties of H-Beta Zeolite as Probed by Bases with Proton Affinity in the 118-204 Kcal Mol^{-1} Range: A FTIR Investigation. *J. Phys. Chem. B* **1997,** *101*, 4740-4751.

(46) Bordiga, S.; Regli, L.; Cocina, D.; Lamberti, C.; Bjorgen, M.; Lillerud, K. P. Assessing the Acidity of High Silica Chabazite H-SSZ-13 by FTIR Using CO as Molecular Probe: Comparison with H-SAPO-34. *J. Phys. Chem. B* **2005,** *109*, 2779-2784.

(47) Bordiga, S.; Roggero, I.; Ugliengo, P.; Zecchina, A.; Bolis, V.; Artioli, G.; Buzzoni, R.; Marra, G.; Rivetti, F.; Spano, G.; Lamberti, C. Characterisation of Defective Silicalites. *J. Chem. Soc., Dalton Trans.* **2000**, 3921-3929.

(48) Bonelli, B.; Zanzottera, C.; Armandi, M.; Esposito, S.; Garrone, E. IR Spectroscopic Study of the Acidic Properties of Alumino-Silicate Single-Walled Nanotubes of the Imogolite Type. *Catal. Today* **2013,** *218-219*, 3-9.

(49) Lamberti, C.; Morterra, C.; Bordiga, S.; Cerrato, G.; Scarano, D. Band Resolution Techniques and Fourier-Transform Infrared-Spectra of Adsorbed Species. *Vib. Spectrosc.* **1993,** *4*, 273-284.

(50) Glatzel, P.; Weng, T.-C.; Kvashnina, K.; Swarbrick, J.; Sikora, M.; Gallo, E.; Smolentsev, N.; Mori, R. A. Reflections on Hard X-Ray Photon-in/Photon-out Spectroscopy for Electronic Structure Studies. *J. Electron Spectrosc. Relat. Phenom.* **2013,** *188*, 17-25.

(51) Lamble, G.; Moen, A.; Nicholson, D. G. Structure of the Diamminecopper(I) Ion in Solution. An X-Ray Absorption Spectroscopic Study. *J. Chem. Soc. Farady Trans.* **1994,** *90*, 2211-2213.

(52) Mathisen, K.; Stockenhuber, M.; Nicholson, D. G. In Situ XAS and IR Studies on Cu:SAPO-5 and Cu:SAPO-11: The Contributory Role of Monomeric Linear Copper(I) Species in the Selective Catalytic Reduction of NO_x by Propene. *Phys. Chem. Chem. Phys.* **2009,** *11*, 5476-5488.

(53) Gomez-Lor, B.; Iglesias, M.; Cascales, C.; Gutierrez-Puebla, E.; Monge, M. A. A Diamine Copper(I) Complex Stabilized in Situ within the Ferrierite Framework. Catalytic Properties. *ACS Chem. Mater.* **2001,** *13*, 1364-1368.

(54) Gallo, E.; Lamberti, C.; Glatzel, P. Investigation of the Valence Electronic States of Ti(IV) in Ti Silicalite-1 Coupling X-Ray Emission Spectroscopy and Density Functional Calculations. *Phys. Chem. Chem. Phys.* **2011,** *13*, 19409-19419.

(55) Gallo, E.; Bonino, F.; Swarbrick, J. C.; Petrenko, T.; Piovano, A.; Bordiga, S.; Gianolio, D.; Groppo, E.; Neese, F.; Lamberti, C.; Glatzel, P. Preference Towards Five-Coordination in Ti Silicalite-1 Upon Molecular Adsorption. *ChemPhysChem* **2013,** *14*, 79-83.

(56) Glatzel, P.; Bergmann, U. High Resolution 1s Core Hole X-Ray Spectroscopy in 3d Transition Metal Complexes - Electronic and Structural Information. *Coord. Chem. Rev.* **2005,** *249*, 65-95.

(57) Vegelius, J. R.; Kvashnina, K. O.; Klintenberg, M.; Soroka, I. L.; Butorin, S. M. Cu $K\beta_{2,5}$ X-Ray Emission Spectroscopy as a Tool for Characterization of Monovalent Copper Compounds. *J. Anal. At. Spectrom.* **2012,** *27*, 1882-1888.

(58) ADF2012, SCM, Theoretical Chemistry, Vrije Universiteit, Amsterdam, The Netherlands: http://www.scm.com

(59) te Velde, G.; Bickelhaupt, F. M.; Baerends, E. J.; Guerra, C. F.; Van Gisbergen, S. J. A.; Snijders, J. G.; Ziegler, T. Chemistry with ADF. *J. Comput. Chem.* **2001,** *22*, 931-967.

(60) Busca, G.; Lietti, L.; Ramis, G.; Berti, F. Chemical and Mechanistic Aspects of the Selective Catalytic Reduction of NO_x by Ammonia over Oxide Catalysts: A Review. *Appl. Catal. B-Environ.* **1998,** *18*, 1-36.

(61) Pant, A.; Schmieg, S. J. Kinetic Model of NO_x SCR Using Urea on Commercial Cu-Zeolite Catalyst. *Ind. Eng. Chem.* **2011,** *50*, 5490-5498.

(62) Davydov, A. The Nature of Oxide Surface Centers. In *Molecular Spectroscopy of Oxide Catalyst Surfaces*, John Wiley & Sons, Ltd: 2003; pp 27-179.

(63) Peri, J. B. Infrared Study of OH and NH_2 Groups on the Surface of a Dry Silica Aerogel. *J. Phys. Chem.* **1966,** *70*, 2937-2945.

(64) Folman, M. Infra-Red Studies of NH_3 Adsorption on Chlorinated Porous Vycor Glass. *Trans. Faraday Soc.* **1961,** *57*, 2000-2006.

(65) Coluccia, S.; Garrone, E.; Borello, E. Infrared Spectroscopic Study of Molecular and Dissociative Adsorption of Ammonia on Magnesium Oxide, Calcium Oxide and Strontium Oxide. *J. Chem. Soc., Faraday Trans. 1* **1983,** *79*, 607-613.

(66) Larrubia, M. A.; Ramis, G.; Busca, G. An FT-IR Study of the Adsorption of Urea and Ammonia over V_2O_5-MoO_3-TiO_2 SCR Catalysts. *Appl. Catal. B: Environ.* **2000,** *27*, L145-L151.

(67) Szanyi, J.; Kwak, J. H.; Zhu, H.; Peden, C. H. F. Characterization of Cu-SSZ-13 NH_3 SCR Catalysts: An in Situ FTIR Study. *Phys. Chem. Chem. Phys.* **2013,** *15*, 2368-2380.

(68) Spoto, G.; Zecchina, A.; Bordiga, S.; Ricchiardi, G.; Martra, G.; Leofanti, G.; Petrini, G. Cu(I)-ZSM-5 Zeolites Prepared by Reaction of H-ZSM-5 with Gaseous CuCl: Spectroscopic Characterization and Reactivity Towards Carbon Monoxide and Nitric Oxide. *Appl. Catal. B-Environ.* **1994,** *3*, 151-172.

Supporting Information

Interaction of NH_3 with Cu-SSZ-13 Catalyst: a Complementary FTIR, XANES and XES Study

Filippo Giordanino[†,±], Elisa Borfecchia[†,±], Kirill A. Lomachenko[†,§], Andrea Lazzarini[†,±], Giovanni Agostini[‡], Erik Gallo[‡], Alexander V. Soldatov[§], Pablo Beato[‖], Silvia Bordiga[,†,±], Carlo Lamberti[†,#,§]*

† Department of Chemistry and INSTM Reference Center, University of Turin, via P. Giuria 7, 10125 Turin, Italy
± NIS Centre of Excellence, University of Turin, Italy
‡ European Synchrotron Radiation Facility, 6, rue Jules Horowitz, B.P. 220, F-38043 Grenoble cedex, France
‖ Haldor Topsøe A/S, Nymøllevej 55, 2800 Kgs. Lyngby, Denmark
CrisDI center of crystallography, University of Turin, Italy
§ Southern Federal University, Zorge street 5, 344090 Rostov-on-Don, Russia

ADDITIONAL INFRARED SPECTRA

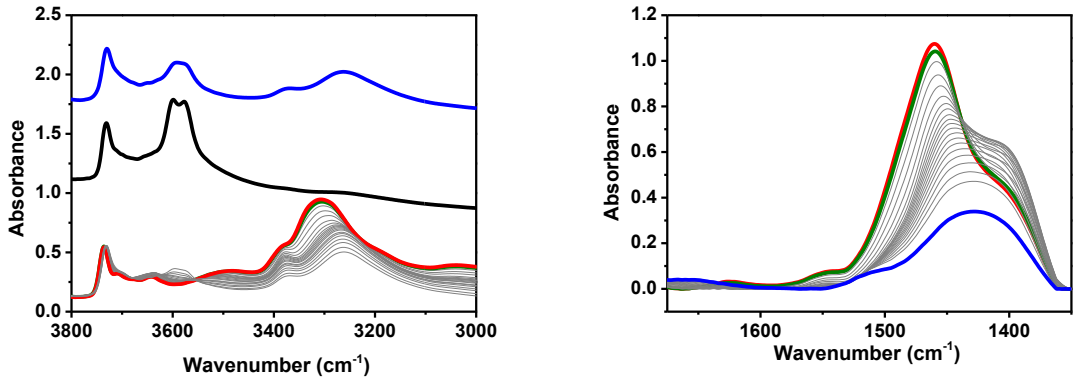

Figure S1. Helium NH_3-TPD over H-SSZ-13. Red curve: maximum NH_3 loading at 100°C; green curve: after He purge at 100°C; grey curves: spectra recorded during TPD experiment in the 120-480°C range; blue curve: final TPD temperature (500°C); black curve: activated sample.

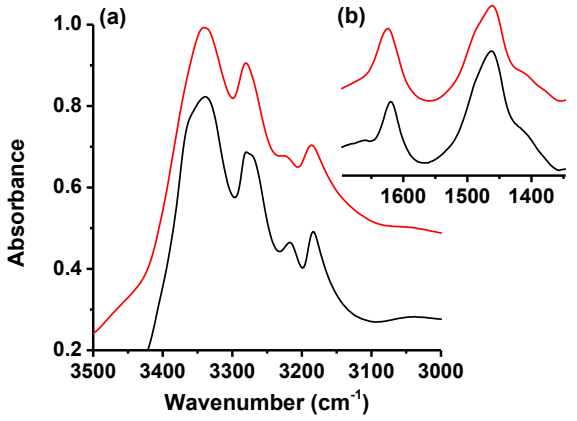

Figure S2. Intermediate coverage of NH_3 adsorbed on *vacuum* (red curve) and O_2-activated Cu-SSZ-13 (black curve). Panel (a): ν(NH) region. Panel (b): δ(NH) region.

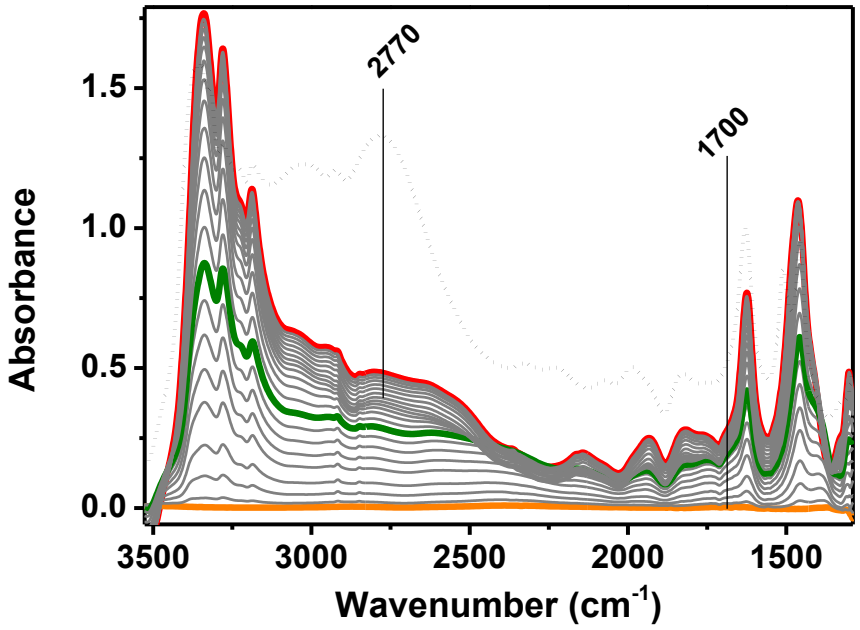

Figure S3. Substracted FTIR spectra of Cu-SSZ-13 at increasing contact time with 1800 ppm of NH_3/He mixture (100 °C). Spectra are plotted in the full spectral range. Orange curve refers to activated sample, red curve refers to highest contact time, *i.e.* highest ammonia loading, grey curves relate to intermediate ammonia loadings. Green curve refers to the total consumption of Brønsted sites ($NH_3/H^+ = 1$). Dotted black curve refers to the spectrum of Cu-SSZ-13 upon NH_3 adsorption at room temperature.

^{27}Al MAS NMR

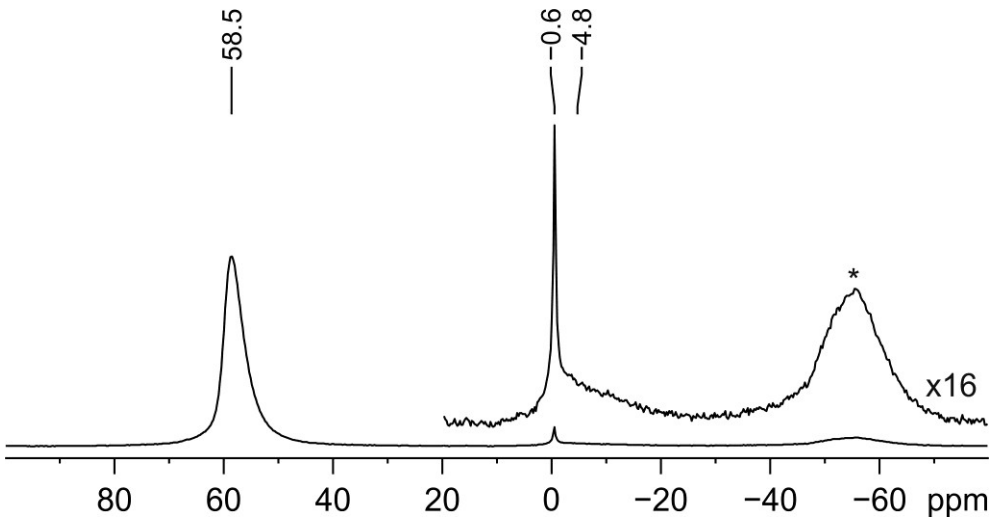

Figure S4. ^{27}Al (104.3 MHz) MAS NMR spectrum of calcined H-SSZ-13 parent material (Si/Al = 12) recorded with a spinning speed of 12 kHz. The asterisk denotes a spinning side band. Main component at 58.5 ppm refers to framework Al atoms in tetrahedral configuration. Integrated areas of -0.6 and -4.8 peaks reveal that the concentration of octahedral-like Al species, *i.e.* extra-framework Al atoms, is lower than 5%.

EXPERIMENTAL DETAILS

The Cu-SSZ-13 sample we used in this work is the same we synthesized and characterized in our previous report[1]. From ICP-OES elemental analysis, it is characterized by Cu/Al = 0.444 and by Si/Al = 13.1.

For FTIR spectroscopy characterization around 15 mg of powdered sample was sieved (140–200 mesh), pressed into self supporting wafer (2.5 ton max) and placed inside a commercial FTIR reactor-cell with KBr windows by AABSPEC (5 #2000-A multimode), operating at atmospheric pressure under flow conditions. Prior to in situ NH_3 desorption experiments sample was dehydrated at 400 °C for 30 minutes by flowing 30 mL/min of 50% O_2/He. After activation the sample was cooled to 100 °C under flowing 50% O_2/He. Ammonia adsorption on dehydrated sample was carried out at 100 °C, by flowing 30 mL/min of 1800 ppm NH3/He for 30 minutes. Desorption experiments were carried out in helium flow by heating up at 5 °C/min from 100 to 500 °C. During TPD experiment, each FTIR spectrum was collected every 20 °C with a resolution of 4 cm^{-1} (number of scans equal to 32) on a Perkin Elmer System 2000 infrared spectrophotometer equipped with a MCT detector.

All the X-ray data were collected at the European Synchrotron Radiation Facility (Grenoble, France). The measurements were conducted in the Microtomo reactor cell (developed by the ESRF Sample Environment team), which allowed to precisely control the gas composition and the temperature inside. The powdered Cu-SSZ-13 sample was pressed in a self supporting pellet, which was then inserted in the cell. The pellet weight was optimized in order to obtain the best S/N ratio for XAS measurements in transmission mode ($\Delta\mu x \approx 0.5$ with the estimated total absorption of 2.4), resulting in ~ 110 mg per 1.3 cm^2 pellet. The gas-flow setup used in the experiment consisted of the

three main channels, each of them connected by stainless steel tubes to gas bottles with oxygen, ammonia and helium. Activation in oxygen was performed by flowing 50% O_2 in He. Ammonia adsorption was carried out at 120 °C, by flowing a mixture of 1300 ppm of NH_3/He. In both cases the total flow rate was 50 ml/min. Activation in vacuum conditions has been carried out at 400°C employing a grease-free set-up in order to prevent the possible reduction of copper centers by hydrocarbons contaminations.

Conventional Cu K-edge XANES measurements were carried out at the BM23 beamline in transmission mode using double-crystal Si (111) monochromator for the incident energy scan and ionization chambers for the detection of incident and transmitted photons. The chambers were filled with the He/Ar mixture up to 2.2 bar with the partial pressure of argon of 0.1 and 0.3 bar for I_0 and I_1 chambers respectively. For the accurate edge energy calibration, a copper foil was measured simultaneously with all the acquired spectra using a third ionization chamber I_2.[2,3] Acquisition time was around 5 min for each of the collected XANES spectra.

Cu K-edge HERFD XANES and Kβ XES measurements were performed at the ID26 beamline. HERFD XANES spectra were acquired in fluorescence mode detecting only photons whose energy corresponded to the maximum intensity of the Cu $K\beta_{1,3}$ emission line (roughly 8906 eV). Such a selection was made using (800) reflection of a single Ge (100) analyzer crystal set up in vertical Rowland geometry. The crystal was spherically bent following the Johann scheme to focus the fluorescence radiation on the APD detector. For the incident beam a flat double-crystal Si (311) monochromator was employed. To measure XES the incident energy was set to 9050 eV while scans over the emitted energy were performed using the same analyzer crystal as for HERFD XANES. Integration time for each of the emission spectra was around 3 hours, whereas each of the in situ HERFD XANES presented is an average of 15 1-minute scans.

All the acquired X-ray absorption spectra were normalized to unity edge jump using the Athena software from the Demeter package.[4] HERFD XANES spectra were subsequently smoothened by the 2nd order Savitzky-Golay filter employing a 20-point window.[5] XES spectra were smoothened using the same filter with a 10-point window. Background subtraction for the XES data and the XANES pre-edge features was carried out in the XANES Dactyloscope software modelling the baseline with a polynomial spline.[6]

The ^{27}Al MAS Solid State (SS) NMR spectrum was measured by a single $\pi/2$ pulse experiment (^{27}Al 90°=3 μs, relaxation delay=0.5s, scans=7400) at 9.4 T (^{27}Al=104.3 MHz) on a Bruker Avance II+ 400 spectrometer equipped with a 4 mm o.d. MAS probe (zirconia rotor spun at 12 kHz). ^{27}Al chemical shifts were referenced to a 1M $Al(NO_3)_3$ aqueous solution; i.e., the resonance of $Al(H_2O)_6^{3+}$ set to 0 ppm. The experimental error of the shift was ±0.1 ppm.

COMPUTATIONAL DETAILS

In order to refine the local structure around Cu atom, DFT geometry optimization was performed. Large clusters containing a double 6-ring were cut out of the bulk structure proposed by Deka et al.[7] (space group, R-3m; refined unit cell, a = b = 13.56 Å, c = 14.77 Å), as shown in Figure S5. During the optimization, the not greenish blue-highlighted framework atoms, copper and NH_3 ligands were

allowed to move freely without any symmetry restriction. Coordinates of the greenish blue-highlighted Si and O atoms were frozen in order to simulate the interaction of the d6 ring with the framework, which is not likely to be significantly perturbed far away from the Cu position. In order to avoid convergence problems caused by dangling bonds, hydrogen atoms were added to the terminal oxygens (not shown in Figure S5).

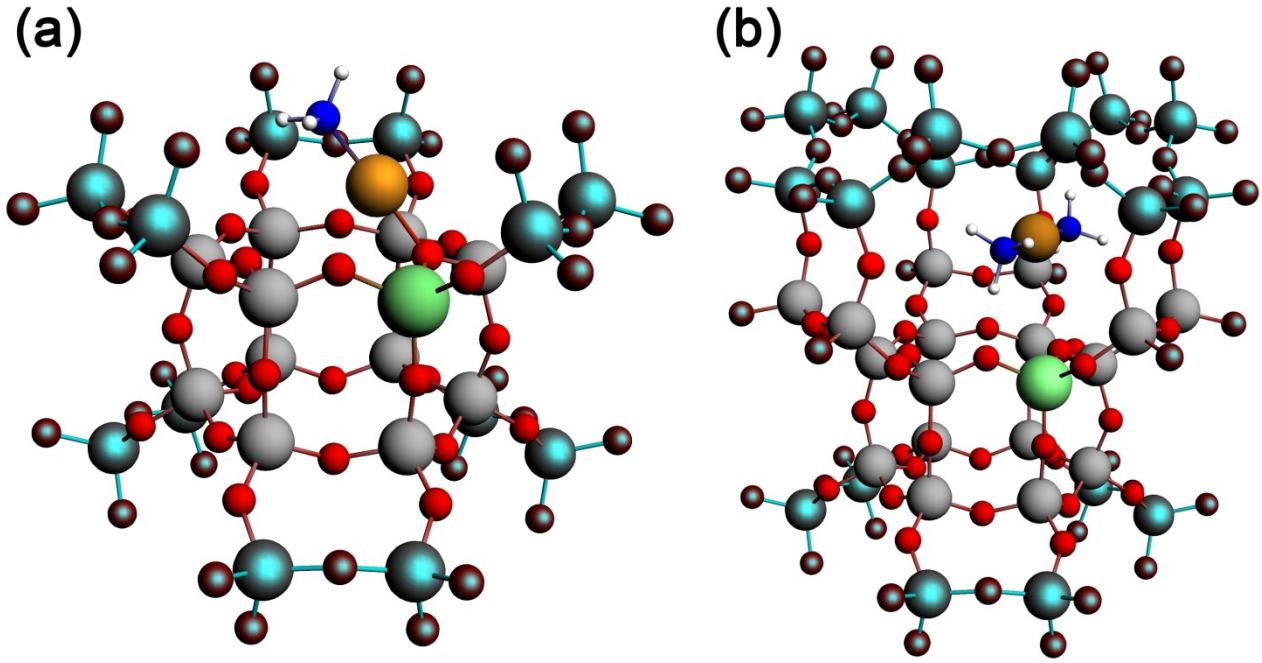

Figure S5. Resulting cluster models for the cases of one (a) and two (b) NH_3 molecules adsorbed on copper. Color code: orange – Cu, green – Al, grey – Si, red – O, blue – N, white – H. Coordinates of the highlighted (greenish blue) atoms were frozen during the geometry optimization.

Geometry optimization was performed using the ADF2012 software. Slater-type TZ2P basis set was employed for all atoms together with the frozen core approximation (up to 2p frozen for Cu, Si and Al, 1s frozen for O). In order to account for exchange correlation effects, PBE functional was applied. Relativistic effects, though small in this system of light elements, were dealt by means of the scalar ZORA approximation. Obtained convergence for both structures was better than 0.00007 Hartree for the energy and better that 0.003 Hartree/Angstrom for the largest energy gradient.

REFERENCES

(1) Giordanino, F.; Vennestrom, P. N. R.; Lundegaard, L. F.; Stappen, F. N.; Mossin, S. L.; Beato, P.; Bordiga, S.; Lamberti, C. Characterization of Cu-Exchanged SSZ-13: A Compared FTIR, UV-Vis and EPR Study with Cu-ZSM-5 and Cu-β with Similar Si/Al and Cu/Al Ratios. *Dalton Trans.* **2013,** *42*, 12741-12761.

(2) Bordiga, S.; Groppo, E.; Agostini, G.; van Bokhoven, J. A.; Lamberti, C. Reactivity of Surface Species in Heterogeneous Catalysts Probed by in Situ X-Ray Absorption Techniques. *Chem. Rev.* **2013,** *113*, 1736-1850.

(3) Lamberti, C.; Bordiga, S.; Bonino, F.; Prestipino, C.; Berlier, G.; Capello, L.; D'Acapito, F.; Xamena, F.; Zecchina, A. Determination of the Oxidation and Coordination State of Copper on

Different Cu-Based Catalysts by XANES Spectroscopy in Situ or in Operando Conditions. *Phys. Chem. Chem. Phys.* **2003,** *5*, 4502-4509.

(4) Ravel, B.; Newville, M. Athena, Artemis, Hephaestus: Data Analysis for X-Ray Absorption Spectroscopy Using Ifeffit. *J. Synchrotron Rad.* **2005,** *12*, 537-541.

(5) Savitzky, A.; Golay, M. J. E. Smoothing and Differentiation of Data by Simplified Least Squares Procedures. *Anal. Chem.* **1964,** *36*, 1627-1639.

(6) Klementiev, K. V. XANES dactyloscope for Windows, freeware: www.cells.es/Beamlines/CLAESS/software/xanda.html

(7) Deka, U.; Juhin, A.; Eilertsen, E. A.; Emerich, H.; Green, M. A.; Korhonen, S. T.; Weckhuysen, B. M.; Beale, A. M. Confirmation of Isolated Cu^{2+} Ions in SSZ-13 Zeolite as Active Sites in NH_3-Selective Catalytic Reduction. *J. Phys. Chem. C* **2012,** *116*, 4809-4818.